that extended Hückel calculations[16] also suggest that the lowest energy transitions are of the nπ^* type. This method is undoubtedly even less reliable for predicting energies of nπ^* type transitions.

Conclusions

We believe that as a result of this work the low-energy allowed $\pi\pi^*$ transitions, as well as some of the low-energy forbidden $\pi\pi^*$ transitions, have now been identified in the spectra of the oxocarbon dianions **1–4** and are reasonably well understood. Calculations indicate that many nπ^* transitions are also present at low energies, but their identification in experimental spectra is difficult.

Acknowledgment. The authors acknowledge support from the U.S. Public Health Service (GM-21153) and from the National Science Foundation (CHE 78-5005). We are grateful to Professors M. C. Zerner and F. H. Harris for their respective contributions to our computer program.

Experimental and Theoretical Evidence for Double Bonds between Metal Atoms. Dinuclear Alkoxo-Bridged Ditungsten(IV,IV) Complexes, $W_2Cl_4(OR)_4(ROH)_2$

Lori Beth Anderson,[1a,c] F. Albert Cotton,*[1b] David DeMarco,[1a] Anne Fang,[1b] William H. Ilsley,[1b] Brian W. S. Kolthammer,[1b] and Richard A. Walton*[1a]

Contribution from the Department of Chemistry, Purdue University, West Lafayette, Indiana 47907, and Texas A&M University, College Station, Texas 77843.

Received March 18, 1981. Revised Manuscript Received April 24, 1981

Abstract: The two compounds of general formula $W_2Cl_4(OR)_4(HOR)_2$ with R = CH_3 (**1**) and R = C_2H_5 (**2**) have been prepared from W_2(2,4-dimethyl-6-oxopyrimidinate)$_4$. A range of physical techniques, including X-ray crystallography and molecular orbital calculations by the Fenske–Hall method, has been used to characterize them, especially with regard to the bonding between the metal atoms. Crystals of **1** belong to the space group $P2_1/n$ with a = 7.219 (1) Å, b = 9.459 (1) Å, c = 12.047 (1) Å, β = 96.127 (9)°, V = 818.1 (3) Å^3, and Z = 2. Crystals of **2** belong to space group $P2_1/c$ with a = 13.121 (1) Å, b = 9.935 (1) Å, c = 18.737 (2) Å, β = 99.31 (1)°, V = 2410 (4) Å^3, and Z = 4. The structures refined to R_1 = 0.023 and 0.044 and R_2 = 0.033 and 0.055 for **1** and **2**, respectively. The structures are essentially identical, consisting of two distorted octahedra sharing an edge. There is a central $Cl_2W(\mu\text{-}OR)_2WCl_2$ unit which is planar except for the R groups, and the four other RO and ROH ligands are placed above and below this plane to complete the distorted octahedra. On each side of the central plane there is one RO and one ROH ligand which are presumably hydrogen bonded since the O···O distances are ca. 2.49 Å. The tungsten–tungsten distances are 2.481 (1) Å in **1** and 2.483 (1) Å in **2**. The metal–metal bond is of formal order 2 and consists of a π bond provided by the HOMO ($11b_u$) and a σ bond provided partly by the highest ($10a_g$) and another ($7a_g$) totally symmetric MO's. The electrochemistry of **2** is consistent with its facile oxidation to the W–W single-bond compound $W_2Cl_4(OEt)_6$. The implications of the present results for a number of other oxo-bridged binuclear systems are briefly discussed.

The question of whether direct metal–metal bonds really exist in bridged dinuclear species, even when magnetic measurements imply that internuclear coupling of electron spins occurs, has been debated for a long time.[2] The compounds we have characterized here, $W_2Cl_4(OR)_4(ROH)_2$, with R = CH_3 and C_2H_5, afford an excellent focus for discussion. The fact that the metal atoms are close together would tend to persuade nearly everyone that there is some direct metal–metal bonding, but there remains the question of whether the bond order is 1 or 2. It could be contended that there is only one direct (presumably σ) bond between the metal atoms and that the spins of the remaining two electrons get coupled by some form of molecular orbital delocalization through the bridging groups. Still other hypotheses are possible. Some nonempirical MO calculations were therefore considered worthwhile not only to give us an understanding of the specific molecules under consideration but for more general reasons.

Our concern with the electronic structures of these molecules was a serendipitous result of an attempt to develop a strategy for the synthesis of the elusive octachloroditungstate(II) anion. We explored the feasibility of converting the quadruply bonded ditungsten complex $W_2(mhp)_4$ (mhp is the anion of 2-hydroxy-6-methylpyridine) to $[W_2Cl_8]^{4-}$ through its reaction with gaseous hydrogen chloride in alcohol solvents.[3] Although unsuccessful in this our original objective, we did discover that this reaction is a very convenient synthetic route to the class of dinuclear complexes which were first formulated by Clark and Wentworth[4] as the green tungsten(III) complexes $W_2Cl_4(OR)_2(ROH)_4$. Following the work of Clark and Wentworth, others,[5,6] using different synthetic procedures, described dark green tungsten(IV) compounds $W_2Cl_4(OR)_4(ROH)_2$, the stoichiometric formulation of which differs from $W_2Cl_4(OR)_2(ROH)_4$ by only two hydrogen atoms. Since the properties of these materials are so similar,[3-6] we considered it likely that they actually constitute a single class of complex, either being derivatives of tungsten(III) or tungsten(IV).

The course of the present investigation therefore shaped itself to the following objectives: (1) to confirm as far as is possible that the spectroscopic properties of the samples from the different procedures are identical; (2) to characterize these molecules structurally by x-ray crystallography; (3) to carry out theoretical studies of the tungsten–tungsten bonding by using the structural data. Our results confirm that these complexes are all members

---

[1] (a) Purdue University. (b) Texas A&M University. (c) 1980 Summer undergraduate research participant from Grove City College, PA.

[2] See, for example: Cotton, F. A. *Rev. Pure Appl. Chem.* **1967**, *17*, 25.

[3] DeMarco, D.; Nimry, T.; Walton, R. A. *Inorg. Chem.* **1980**, *19*, 575.

[4] Clark, P. W.; Wentworth, R. A. D. *Inorg. Chem.* **1969**, *8*, 1223.

[5] Reagan, W. J.; Brubaker, C. H., Jr., *Inorg. Chem.* **1970**, *9*, 827.

[6] Seifert, H. J.; Petersen, F.; Wohrmann, H. *J. Inorg. Nucl. Chem.* **1973**, *35*, 2735.

0002-7863/81/1503-5078$01.25/0

of the same family of tungsten(IV) complexes and that W═W double bonds are present. This bond order is far less prevalent than M≡M and M≣M bonds.[7]

Experimental Section

All chemical operations were conducted in an atmosphere of nitrogen by using standard Schlenk techniques. 2,4-Dimethyl-6-hydroxypyrimidine (Hdmhp) was purchased from Aldrich Chemical Co., Inc., and used as received. $W(CO)_6$ and tri-*n*-propylphosphine were purchased from Strem Chemical Co. Methanol and ethanol were dried over molecular sieves and purged with nitrogen prior to use. All other solvents were dried and distilled.

Preparation of $W_2(dmhp)_4$. $W_2(dmhp)_4$ was prepared by using a procedure similar to that previously reported.[8] In a typical reaction, 3.5 g of $W(CO)_6$ and 1.8 g of Hdmhp were placed in a three-neck 300-mL round-bottom flask. A 150-mL sample of an *o*-dichlorobenzene–hexane mixture (10:1) was added, and the solution was refluxed for 12 h. The resulting deep red solution was then vacuum distilled to small volume. The resulting red product was collected, washed with hexanes, and dried under vacuum. Yields of 85–90% were obtained in this manner.

Preparation of Crystalline $W_2Cl_4(OMe)_4(MeOH)_2$ (1). Tri-*n*-propylphosphine (0.5 mL) was syringed into a suspension of 0.5 g of $W_2(dmhp)_4$ in 30 mL of methanol. Gaseous anhydrous hydrogen chloride was bubbled through the resulting mixture. After a short time, the solution turned a deep purple color. At this point the flow of hydrogen chloride was stopped and the solution was filtered. The air-sensitive purple filtrate was allowed to stand undisturbed for 12 h. After this time, dark green crystals of $W_2Cl_4(OMe)_4(MeOH)_2$ were filtered off, washed with methanol and diethyl ether, and dried under vacuum. These crystals were found to be suitable for an X-ray structure analysis.

Preparation of Crystalline $W_2Cl_4(OEt)_4(EtOH)_2$ (2). An alcohol exchange reaction of $W_2Cl_4(OMe)_4(MeOH)_2$ with ethanol was carried out by heating a mixture of these reagents. Crystals suitable for an X-ray structure analysis were grown from a $CHCl_3$–EtOH mixture. Samples of this complex were also prepared by the method of Reagan and Brubaker[5] in which ethanol is reacted with tungsten(IV) chloride.

Spectroscopic Characterizations and Electrochemical Measurements. The ^1H NMR spectra of $CDCl_3$ solutions were recorded on a Perkin-Elmer R-32 90-MHz instrument by using Me_4Si as an internal standard. Infrared spectra (4000–200 cm^{-1}) were recorded as Nujol mulls on a Beckman IR-12 spectrophotometer. Far-infrared spectra (500–80 cm^{-1}) were recorded as Nujol mulls between polyethylene plates by using a Digilab FTS-20B Fourier transform interferometer. Electronic absorption spectra were measured on $CHCl_3$ solutions by using Cary 14 and Cary 17B spectrophotometers and on solid samples by using a Beckman DU-2 spectrophotometer.

Electrochemical measurements were made on dichloromethane solutions containing 0.2 M tetra-*n*-butylammonium hexafluorophosphate (TBAH) as supporting electrolyte. $E_{1/2}$ values (taken as $(E_{p,a} + E_{p,c})/2$) are referenced to the saturated potassium chloride calomel electrode (SCE) at 22 ± 2 °C and are uncorrected for junction potentials. Cyclic voltammetry experiments were performed by using a BioAnalytical Systems Inc. Model CV-1A instrument in conjunction with a Hewlett-Packard Model 7035B x-y recorder. Potential control for coulometric experiments was maintained with a potentiostat purchased from BioAnalytical Systems Inc. All voltammetric measurements were made at a platinum bead electrode in solutions deaerated with a stream of dry nitrogen gas.

X-ray Structure Determinations. Compound 1. A well-formed regularly shaped crystal of dimensions 0.13 × 0.18 × 0.20 mm was attached to the end of a thin glass fiber, by using epoxy glue. The crystal was transferred to an Enraf-Nonius CAD-4 automated diffractometer where a least-squares analysis of the setting angles of 25 reflections (26° ≤ 2θ ≤ 32°), automatically located and centered, provided accurate unit-cell parameters (Table I). Systematic absences of $h,0,l$ for $h + l \neq 2n$ and $0,k,0$ for $k \neq 2n$ suggested the space group $P2_1/n$. Intensity data were collected[9] at ambient temperature (ca. 22 °C) in the range $0° < 2\theta \leq 45°$ by using the CAD-4 parameters and procedures summarized in Table I. A total of 1060 unique reflections were measured of which 903 had intensity, I, exceeding $3\sigma(I)$ and were considered observed. The data set was corrected for Lorentz and polarization effects, and an empirical absorption correction based on the ψ-scan method (ψ = 0–360° every 10° for χ values near 90°) was made.

Table I. Crystallographic Data and Enraf-Nonius CAD-4 Data Collection Parameters

	1	2
formula	$W_2Cl_4O_6C_6H_{20}$	$W_2Cl_4O_6C_{12}H_{32}$
M_r	697.7	779.9
space group	$P2_1/n$	$P2_1/c$
a, Å	7.219 (1)	13.121 (1)
b, Å	9.459 (1)	9.935 (1)
c, Å	12.047 (1)	18.737 (2)
β, Å	96.127 (9)	99.31 (1)
V, Å^3	818.1 (3)	2410 (1)
Z	2	4
ρ_C, g/cm^3	2.832	2.149
μ(Mo Kα), cm^{-1}	155.5	105.6
radiatn	graphite monochromated Mo Kα (λ = 0.71073 Å)	
range 2θ, deg	0–45	0–50
scan type	ω–2θ	ω–2θ
scan width (Δw), deg	0.75 + 0.35 tan θ	0.55 + 0.35 tan θ
aperature width, deg	1.50 + 1.0 tan θ	1.50 + 1.0 tan θ
prescan rejection	2.0	2.0
prescan acceptance	0.02	0.02
max counting time, s	40	30
no. ψ scans	5	9
transmissn factors, min	0.76	0.57
max	0.99	1.00
av	0.90	0.74
no. of unique data	1060	4483
no. of data $I > 3\sigma(I)$	903	3126
p	0.05	0.05
no. of variables	82	218
R_1	0.023	0.044
R_2	0.033	0.055
esd	1.066	1.655
extinction coeff	1.59 × 10^{-7}	1.38 × 10^{-7}
largest shift[a]	0.06	0.01
largest peak[b]	0.90	2.50

[a] In final refinement cycle. [b] In final difference Fourier, e/Å^3.

The structure was solved by Patterson and Fourier methods and refined[10] by full-matrix least squares. A Patterson synthesis provided one tungsten atom on a general (fourfold) position, consistent with the expected results of $Z = 2$ with the molecule located at a site with crystallographic inversion symmetry. Three cycles of isotropic refinement produced values of $R_1 = 0.210$ and $R_2 = 0.304$, where R_i are defined as $R_1 = \sum||F_o| - |F_c||/\sum|F_o|$ and $R_2 = [\sum w(|F_o| - |F_c|)^2/\sum w|F_o|^2]^{1/2}$. The remaining nonhydrogen atoms were located by using a difference Fourier map, and least-squares refinement of the isotropic model gave $R_1 = 0.058$ and $R_2 = 0.074$. Following convergence of anisotropic least-squares refinement, a difference Fourier synthesis produced no positions suitable for hydrogen atoms. An extinction correction was made, and during the last stages of refinement the $1,2,\bar{1}$ reflection with $|F_o| = 12.5$ and $|F_c| = 3.2$ was omitted. The final cycle of refinement yielded values of $R_1 = 0.023$ and $R_2 = 0.033$. The error in an observation of unit weight was 1.07, and the largest shift/error in the final cycle was 0.06. A final difference synthesis exhibited peaks as high as 0.90 e/Å^3 in the vicinity of the W atoms and random fluctuations not greater than 0.50 e/Å^3 elsewhere.

Compound 2. Crystals of this substance were glued to the end of thin fibers and studied on an Enraf-Nonius CAD-4 diffractometer. Those of optimum size were all found to diffract weakly and exhibited broad, asymmetric peaks. Larger crystals produced acceptable peak characteristics but presented absorption problems. Finally, a crystal of moderate size was chosen with dimensions of 0.35 × 0.35 × 0.30 mm. Unit-cell parameters were obtained on a CAD-4 diffractometer as above and are listed in Table I. Systematic absences in $h,0,l$ for $l \neq 2n$ and in $0,k,0$ for $k \neq 2n$ indicated the space group $P2_1/c$. Intensity data were collected as explained above except that the range was extended to 2θ = 50°. A total of 4483 unique data were collected of which 3126 had $I > 3\sigma(I)$ and were considered observed. Standard Lorentz and polarization corrections were made as well as an empirical absorption correction based on ψ scans (vide supra).

---

(7) Cotton, F. A.; Walton, R. A. "Multiple Bonds Between Metal Atoms"; Wiley: New York, 1981; in press.

(8) Cotton, F. A.; Niswander, R. H.; Sekutowski, J. C. *Inorg. Chem.* **1979**, *18*, 1152.

(9) Bino, A.; Cotton, F. A.; Fanwick, P. E. *Inorg. Chem.* **1979**, *18*, 3558.

(10) All crystallographic computing was performed on a PDP 11/45 or PDP 11/60 computer at the Molecular Structure Corp., College Station, TX, employing the Enraf-Nonius Structure Determination Package with local modifications.

Table II. Positional and Thermal Parameters and Their Estimated Standard Deviations for $W_2Cl_4(OCH_3)_4(HOCH_3)_2$ (1)

atom	*x*	*y*	*z*	*B*(1,1)	*B*(2,2)	*B*(3,3)	*B*(1,2)	*B*(1,3)	*B*(2,3)
W(1)	0.07304 (4)	0.11474 (3)	0.02907 (3)	2.47 (1)	1.49 (1)	2.41 (1)	−0.21 (1)	0.37 (1)	−0.22 (1)
Cl(1)	0.2551 (3)	0.2851 (3)	−0.0564 (2)	4.0 (1)	2.7 (1)	5.1 (1)	−0.86 (9)	1.0 (1)	0.65 (9)
Cl(2)	0.0768 (4)	0.2629 (3)	0.1899 (2)	4.8 (1)	3.4 (1)	3.3 (1)	0.44 (9)	0.1 (1)	−1.40 (9)
O(1)	0.0871 (8)	0.0109 (7)	−0.1174 (5)	3.3 (2)	3.4 (3)	3.5 (3)	−0.2 (2)	0.9 (2)	−0.3 (2)
O(2)	−0.1626 (8)	0.2145 (6)	−0.0380 (5)	2.4 (2)	1.8 (2)	3.7 (3)	0.3 (2)	−0.0 (2)	0.1 (2)
O(3)	0.2978 (7)	0.0193 (6)	0.0947 (5)	2.2 (2)	2.2 (2)	3.5 (3)	−0.0 (2)	−0.4 (2)	−0.1 (2)
C(1)	0.058 (2)	0.0565 (12)	−0.2332 (8)	6.0 (5)	4.7 (5)	2.6 (4)	−0.6 (5)	0.7 (4)	1.2 (4)
C(2)	−0.215 (1)	0.3649 (9)	−0.0348 (9)	3.8 (4)	1.9 (4)	5.0 (5)	1.3 (3)	−0.0 (4)	−0.0 (3)
C(3)	0.475 (1)	0.0756 (11)	0.1510 (9)	2.7 (4)	3.8 (4)	5.3 (5)	−1.1 (4)	−0.6 (4)	0.2 (4)

[a] The form of the anisotropic thermal parameter is $\exp[-0.25\{h^2a^{*2}B(1,1) + k^2b^{*2}B(2,2) + l^2c^{*2}B(3,3) + 2hka^*b^*B(1,2) + 2hla^*c^*B(1,3) + 2klb^*c^*B(2,3)\}]$ where *a*, *b*, and *c* are reciprocal lattice constants. [b] Estimated standard deviations in the least significant digits are shown in parentheses.

Table III. Positional and Thermal Parameters and Their Estimated Standard Deviations for $W_2Cl_4(OCH_2CH_3)_4(HOCH_2CH_3)_2$ (2)

atom	*x*	*y*	*z*	*B*(1,1)	*B*(2,2)	*B*(3,3)	*B*(1,2)	*B*(1,3)	*B*(2,3)
W(1)	0.19247 (3)	0.04731 (4)	0.22435 (2)	2.98 (1)	2.46 (2)	4.34 (2)	−0.43 (1)	0.27 (1)	0.01 (2)
W(2)	0.30147 (3)	0.25244 (4)	0.24460 (3)	3.00 (2)	2.37 (2)	5.52 (2)	−0.37 (1)	0.19 (2)	0.01 (2)
Cl(1)	0.4267 (2)	0.3589 (3)	0.1842 (2)	3.7 (1)	5.0 (1)	13.1 (2)	−0.5 (1)	1.9 (1)	3.3 (2)
Cl(2)	0.3212 (3)	0.4350 (3)	0.3288 (2)	8.2 (2)	3.2 (1)	8.4 (2)	−0.1 (1)	−1.6 (2)	−1.4 (1)
Cl(3)	0.1710 (3)	−0.1348 (3)	0.1400 (2)	8.1 (2)	3.6 (1)	5.8 (2)	−0.5 (1)	−0.9 (1)	−1.0 (1)
Cl(4)	0.0669 (2)	−0.0598 (3)	0.2845 (2)	4.0 (1)	5.4 (1)	8.1 (2)	−0.8 (1)	1.4 (1)	2.0 (1)
O(1)	0.2952 (5)	0.1160 (7)	0.1633 (4)	4.2 (3)	2.8 (3)	5.0 (3)	0.1 (3)	1.3 (3)	0.3 (3)
O(2)	0.1978 (5)	0.1846 (7)	0.3046 (4)	3.7 (3)	3.2 (3)	4.6 (3)	0.2 (3)	0.4 (3)	−0.5 (3)
O(3)	0.4106 (5)	0.1509 (7)	0.3049 (4)	3.8 (3)	3.6 (3)	6.1 (4)	−1.1 (3)	−0.9 (3)	0.7 (3)
O(4)	0.1892 (5)	0.3590 (7)	0.1825 (4)	4.0 (3)	3.0 (3)	4.4 (3)	−0.2 (3)	0.1 (3)	0.8 (3)
O(5)	0.3045 (5)	−0.0577 (7)	0.2869 (4)	4.0 (3)	3.9 (3)	3.3 (3)	−0.7 (3)	0.2 (3)	0.5 (3)
O(6)	0.0827 (5)	0.1507 (7)	0.1642 (4)	3.2 (3)	4.0 (3)	4.9 (3)	−0.9 (3)	−0.3 (3)	0.5 (3)
C(1)	0.3750 (13)	0.052 (2)	0.1314 (10)	11.1 (8)	6.4 (8)	11.1 (9)	0.4 (8)	6.5 (6)	−0.3 (8)
C(2)	0.3646 (16)	0.075 (2)	0.0547 (10)	15 (1)	13 (1)	6.8 (8)	0 (1)	5.2 (8)	1 (1)
C(3)	0.1179 (11)	0.246 (1)	0.3379 (8)	8.1 (7)	6.2 (7)	7.0 (7)	2.6 (6)	3.4 (5)	−0.3 (6)
C(4)	0.1422 (16)	0.215 (2)	0.4165 (10)	15 (1)	15 (2)	5.8 (8)	1 (1)	4.3 (8)	−1 (1)
C(5)	0.5151 (9)	0.194 (1)	0.3408 (8)	3.9 (5)	5.6 (6)	8.0 (8)	−1.1 (5)	−3.0 (5)	0.2 (6)
C(6)	0.5236 (12)	0.163 (2)	0.4196 (10)	7.8 (8)	9 (1)	8.5 (9)	1.2 (8)	−2.8 (7)	−3.0 (8)
C(7)	0.1839 (9)	0.501 (1)	0.1624 (7)	4.5 (5)	2.6 (4)	6.5 (6)	0.4 (4)	−0.4 (5)	1.1 (5)
C(8)	0.1557 (17)	0.511 (2)	0.0822 (10)	19 (2)	3.8 (6)	7.2 (9)	−0.5 (9)	1 (1)	1.6 (7)
C(9)	0.3057 (8)	−0.197 (1)	0.3114 (7)	3.6 (4)	1.8 (4)	6.3 (6)	0.2 (3)	0.4 (4)	1.0 (4)
C(10)	0.3240 (11)	−0.201 (1)	0.3924 (8)	7.8 (7)	5.3 (6)	5.2 (7)	−1.5 (6)	0.3 (6)	1.2 (5)
C(11)	−0.0238 (9)	0.111 (1)	0.1329 (7)	4.1 (5)	5.7 (6)	6.4 (7)	−1.5 (5)	−1.5 (5)	0.9 (6)
C(12)	−0.0514 (12)	0.175 (2)	0.0617 (9)	7.4 (8)	11 (1)	7.5 (8)	−2.5 (9)	−3.5 (7)	2.3 (9)

[a] The form of the anisotropic thermal parameter is $\exp[-0.25\{h^2a^{*2}B(1,1) + k^2b^{*2}B(2,2) + l^2c^{*2}B(3,3) + 2hka^*b^*B(1,2) + 2hla^*c^*B(1,3) + 2klb^*c^*B(2,3)\}]$ where *a*, *b*, and *c* are reciprocal lattice constants. [b] Estimated standard deviations in the least significant digits are shown in parentheses.

Table IV. Molecular Orbitals for the Mo_2^{8+} Unit Alone

orb type	orbital	relative energy, eV	symmetry (in C_{2h})	% contribution								
				d_{z^2}	$d_{x^2-y^2}$	d_{xy}	d_{xz}	d_{yz}	S	Px	Py	Pz
σ^*	M_{18}	30.00	b_u	11					27			62
π^*	M_{17}	3.05	b_g					3			97	
π^*	M_{16}	3.05	a_g				3			97		
π	M_{15}	1.59	b_u							89	11	
π	M_{14}	1.59	a_u							11	89	
σ	M_{13}	0.21	a_g	2					13			85
σ^*	M_{12}	−2.45	b_u						67			32
σ	M_{11}	−5.76	a_g	6					83			11
σ^*	M_{10}	−10.00	b_u	88					6			6
π^*	M_9	−9.97	b_g					97			3	
π^*	M_8	−9.97	a_g				97			3		
δ^*	M_7	−11.70	b_u		96	4						
δ^*	M_6	−11.70	a_u		4	96						
δ	M_5	−12.22	a_g		100							
δ	M_4	−12.22	b_g			100						
π	M_3	−13.71	a_u					99			1	
π	M_2	−13.71	b_u				99			1		
σ	M_1	−15.74	a_g	93					3			4

The structure was solved by routine methods. A three-dimensional Patterson map yielded the positions of two W atoms and least-squares refinement of these positions produced initial agreement factors of $R_1 = 0.240$ and $R_2 = 0.329$. A difference Fourier synthesis produced positions for the remaining nonhydrogen atoms and convergence of refinement with an isotropic model led to values of $R_1 = 0.120$ and $R_2 = 0.159$. The inclusion of anisotropic thermal parameters for all atoms in the model followed by a correction for extinction produced the final figures of merit given in Table I. A final difference Fourier map did not supply evidence for hydrogen atom positions; the few remaining electron density peaks were all closely associated with the W atoms and are probably due to inexact corrections for absorption.

Final positional and thermal parameters for **1** and **2** are given in Tables II and III, respectively. Tables of observed and calculated

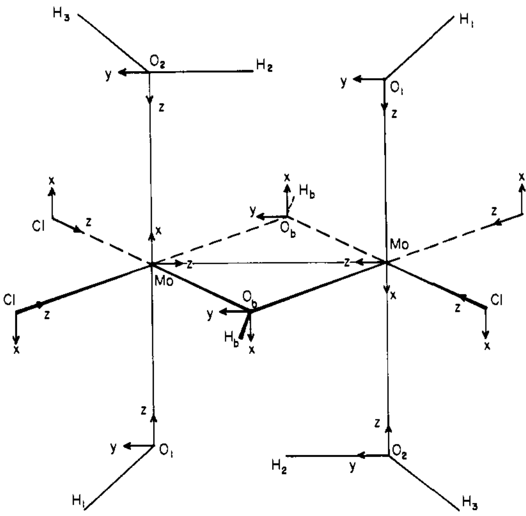

Figure 1. The idealized structure and coordinate systems used in the Fenske-Hall calculations on $Mo_2Cl_4(OH)_4(H_2O)_2$.

structure factors are available as supplementary material.

Molecular Orbital Calculations. The method of Fenske and Hall[11] was used. For practical reasons a molybdenum-containing model system $Mo_2Cl_4(OH)_4(H_2O)_2$ with C_{2h} symmetry was chosen. The coordinate axes used are defined in Figure 1. Bond distances used were averages of those found in compounds **1** and **2**.

As a help in the interpretation of the results for the entire $Mo_2Cl_4(OH)_4(H_2O)_2$ molecule we first treated only the Mo_2^{8+} unit. The results for this simple diatomic species are given in Table IV. The 18 MO's for this isolated unit are designated M_1–M_{18}. In describing the provenance of the MO's for the whole molecule, whose energies are listed in Table V and displayed in Figure 2, we have considered these M_i as a kind of basis set. Also, in the Mulliken population analysis (Table VI), we have given results not only for the individual atoms, as is usual, but in terms of the *d*-based dinuclear orbitals M_1–M_{10}.

Results

Preparations and Spectroscopic Characterizations. In an earlier study we observed[3] that suspensions of $W_2(mhp)_4$ (mhp is the anion of 2-hydroxy-6-methylpyridine) in methanol or ethanol are oxidized by hydrogen chloride to the same green, air-stable, dinuclear complexes which had been formulated by Clark and Wentworth[4] as $W_2Cl_4(OR)_2(ROH)_4$. This would seem to be a general synthetic route starting from other ligand-bridged multiply bonded ditungsten complexes since, in the present investigation, we find that $W_2(dmhp)_4$ (dmhp is the anion of 2,4-dimethyl-6-hydroxypyrimidine) is converted to the methoxy derivative in a crystalline form suitable for a crystal structure determination. As with the earlier studies of Clark and Wentworth,[4] we find that other alkoxy derivatives can be prepared via a simple alcohol-exchange reaction. By this means we were able to form good quality single crystals of the ethoxide derivative.

The synthetic procedures which have been variously reported as affording $W_2Cl_4(OR)_2(ROH)_4$[4] or $W_2Cl_4(OR)_4(ROH)_2$[5,6] are now quite numerous. They include the following: (i) the oxidation of quadruply bonded dinuclear tungsten(II) species in alcoholic HCl solutions;[3] (ii) the reactions of $(Bu_4N)_3W_2Cl_9$ with alcohols;[4] (iii) the electrolytic reduction of alcoholic solutions of WCl_6 in the presence of a little HCl;[6] and (iv) the alcoholysis of WCl_4.[5]

The spectroscopic properties of these various materials indicate that they all belong to the same class of complex. We find that the infrared spectra (4000–600 cm^{-1}) of samples of the ethoxide prepared from $W_2(mhp)_4$, $W_2(dmhp)_4$, and WCl_4 are identical and that these data are in excellent agreement with the data tabulated by Seifert et al.[6] In the low-frequency infrared region (500–200 cm^{-1}) our spectra are very similar to those reported by others[5,6] for both the methoxide and ethoxide. For example, the ν(W–Cl) modes of the ethoxide are at 322 (s), 306 (s), and 292 (ms) cm^{-1}, whereas Seifert et al.[6] report values of 318, 305, and 290 cm^{-1} and Reagan and Brubaker[5] give 319, 302, and 290 cm^{-1} for these same modes.

Table V. Orbital Energies and % Contributions for $Mo_2Cl_4(OH)_4(OH_2)_2$

		% contribution						
orbital	*E*, eV	Mo			Cl	(μ-OH)	(OH_2)	(OH)
$11a_g$	−8.22	88	M_8	(d_{xz})	2		3	4
$9b_g$	−8.91	86	M_4	(d_{xy})	3	6		3
$8a_u$	−9.46	82	M_6	(d_{xy})	5		3	7
$11b_u$	−11.09	77	M_2	(d_{xz})	14	7		
$8b_g$	−12.28	1	M_{17}		97	2		
$7a_u$	−12.70	1	M_3		99			
$10a_g$	−13.27	48	M_1	(d_{z^2})				
		7	M_5	$(d_{x^2-y^2})$	43			
$6a_u$	−13.42	1	M_6		90		3	6
$7b_g$	−13.50	1	M_4		93		1	4
$10b_u$	−13.75	2	M_{10}		85	9		
		3	M_{12}					
$9a_g$	−14.04				86		5	9
$9b_u$	−14.84	12	M_2	(d_{xz})	82			4
$5a_u$	−15.35	14	M_3	(d_{yz})				
		7	M_{14}	(P*y*)	70	2	2	2
$8a_g$	−15.49	4	M_1	(d_{z^2})				
		11	M_5	$(d_{x^2-y^2})$	79	1		
$6b_g$	−15.60	26	M_9	(d_{yz})	65		2	5
$8b_u$	−16.12	4	M_{12}	(S, P*z*)	80		2	5
		5	M_{10}	(d_{z^2})	80		2	6
$7a_g$	−16.85	30	M_1	(d_{z^2})	63	1		
		3	M_5	$(d_{x^2-y^2})$				
$5b_g$	−17.96	2	M_9		4	40		54
$7b_u$	−18.52				14	3	19	60
$6a_g$	−18.97	10	M_8	(d_{xz})	12		20	56
$4b_g$	−19.32	1	M_4		1	33	48	11
		4	M_9					
$4a_u$	−19.76	9	M_6	(d_{xy})	6			84
$6b_u$	−20.00	8	M_2	(d_{xz})		80	2	7
$3a_u$	−21.36	4	M_6		4		92	
$3b_g$	−21.52	5	M_9	(d_{yz})	5	70	5	10
		4	M_{17}	(P*y*)				
$5b_u$	−22.21	4	M_{10}	(d_{z^2})				
		16	M_7	$(d_{x^2-y^2})$	11	67		
$4b_u$	−22.73	7	M_{15}	(P*x*)	2	9	51	30
$2b_g$	−22.88	11	M_4	(d_{xy})	2	32	41	13
$5a_g$	−23.87	9	M_{16}	(P*x*)			51	38
$4a_g$	−24.46	4	M_1	(d_{z^4})				
		12	M_5	$(d_{x^2-y^2})$				
		3	M_{11}	(S)			32	48
$3b_u$	−25.48	7	M_{10}	(d_{z^2})		2	31	50
		8	M_7	$(d_{x^2-y^2})$				
$3a_g$	−25.81	4	M_1			86		
		3	M_5					
		4	M_{11}					
$2a_u$	−26.23	15	M_3	(d_{yz})		80		
		2	M_{14}	(P*y*)				

Table VI. Mulliken Populations of M_i Orbitals and Mulliken Atomic Charges

populations of M_i orbitals				atomic charges	
$M_1(\sigma)$	1.81258	$M_{11}(\sigma)$	0.08321	Mo	1.653
$M_2(\pi)$	1.97905	$M_{12}(\sigma^*)$	0.16242	Cl	−0.499
$M_3(\pi)$	0.71863	$M_{13}(\sigma)$	0.16379	Ob	−0.704
$M_4(\delta)$	0.28505	$M_{14}(\pi)$	0.12935	Hb	0.320
$M_5(\delta)$	0.78493	$M_{15}(\pi)$	0.05079	O	−0.539
$M_6(\delta^*)$	0.30018	$M_{16}(\pi^*)$	0.14389	H_2	0.322
$M_7(\delta^*)$	0.56101	$M_{17}(\pi^*)$	0.10005	H_3	0.312
$M_8(\pi^*)$	0.20530	$M_{18}(\sigma^*)$	0.04481	O_1	−0.660
$M_9(\pi^*)$	0.77646			H_1	0.294
$M_{10}(\sigma^*)$	0.39295				

The ^1H NMR spectral studies reported to date,[4-6] together with our own measurements in the present investigation, show that irrespective of the preparative method used, all samples of the ethoxide in $CDCl_3$ solution exhibit the same methyl and methylene resonances. Methyl triplets are at δ 1.23 and 1.38 (J = 7 Hz for

---

(11) Hall, M. B. and Fenske, R. F. *Inorg. Chem.* **1972**, *11*, 768.

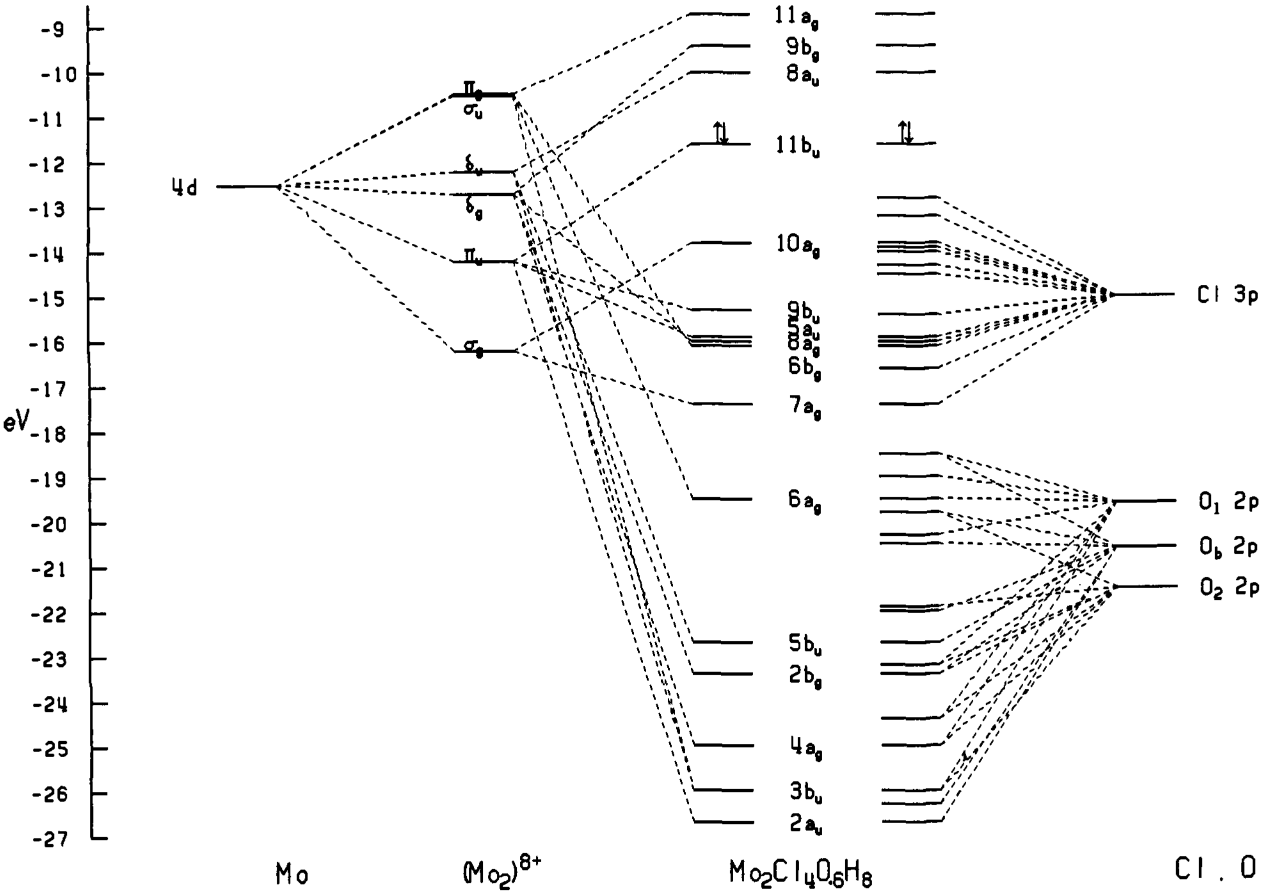

Figure 2. The calculated energy levels for $Mo_2Cl_4(OH)_4(H_2O)_2$.

each) and methylene quartets at δ 4.53 and 5.44 (J = 7 Hz for each). In each case the lower field resonance is half the intensity of the one at higher field and is assignable to OEt bridges.[12] The observation of a single set of methyl and methylene resonances for the terminal ethoxy and ethanol ligands is presumably the result of rapid proton hopping. The one inconsistency in the ^1H NMR spectral data is that while Clark and Wentworth[4] categorically state that they observed no resonance due to hydroxyl protons between δ 20 and −10, Siefert et al.[6] find such a resonance at δ 10.7. We have confirmed the observations of Seifert et al., the hydroxyl resonance occurring as a reasonably sharp resonance at δ 10.72. When these $CDCl_3$ solutions are cooled from room temperature to −55 °C, this resonance broadens considerably but otherwise remains unaffected. Integration of these spectra shows that the EtOH:EtO ratio is 1:2, and this supports the tungsten(IV) formulation $W_2Cl_4(OR)_4(ROH)_2$. We have no explanation for the failure of Clark and Wentworth[4] to observe the hydroxyl proton resonance other than perhaps their use of solutions which were too dilute.

In support of our contention that these products are the same, we have made careful comparisons of their electronic absorption spectra. The spectra we observe for solid samples of $W_2Cl_4(OR)_4(ROH)_2$ (R = Me or Et) resemble closely those exhibited by chloroform solutions of these complexes. Our data are in turn very similar to those reported by Clark and Wentworth[4] for "$W_2Cl_4(OR)_2(ROH)_4$". For example, our measurements on chloroform solutions of the ethoxide showed absorption maxima at 738 and 427 nm with molar extinction coefficients of 166 and 3780 M^{-1} cm^{-1}, respectively. The comparable data reported by Clark and Wentworth[4] are 735 and 426 nm with ε values of 167 and 2980; the only significant difference with our results is in the value of ε for the 426-nm absorption.

A final point concerning the identity of the $W_2Cl_4(OR)_4(ROH)_2$ compounds, however prepared, may conveniently be mentioned here, even though it is not a spectroscopic observation. Seifert et al.[6] made preliminary X-ray crystallographic examinations of their compounds with methoxy and ethoxy groups. For the former they chose a unit cell in the space group $P2_1/c$, but this is equivalent, within experimental error, to our cell in $P2_1/n$. For the ethoxy compound their unit cell in $P2_1/c$ is in agreement with ours. They also report that with use of a very small number of intensity measurements they solved these structures for the metal atom positions and obtained, in each case, W–W distances of about 2.51 Å. There can be no doubt whatever that Seifert et al. had exactly the same compounds as we describe here.

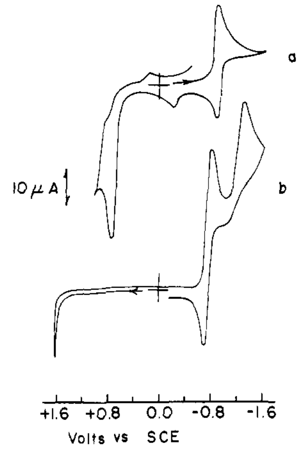

Figure 3. Cyclic voltammograms in 0.2 M tetra-*n*-butylammonium hexafluorophosphate-dichloromethane of (a) $W_2Cl_4(OEt)_4(EtOH)_2$ and (b) $W_2Cl_4(OEt)_6$. Sweep rates for (a) and (b) were 200 mV/s.

Electrochemistry and Redox Behavior of $W_2Cl_4(OEt)_4(EtOH)_2$. Cyclic voltammograms of dichloromethane solutions of this complex are characterized by an irreversible oxidation at $E_{p,a}$ = +0.80 V vs. SCE and a reduction at $E_{1/2}$ = −0.92 V vs. SCE (Figure 3a). That the reduction is electrochemically and chem-

---

[12] Cotton, F. A.; DeMarco, D.; Kolthammer, B. W. S.; Walton, R. A. *Inorg. Chem.*, in press.

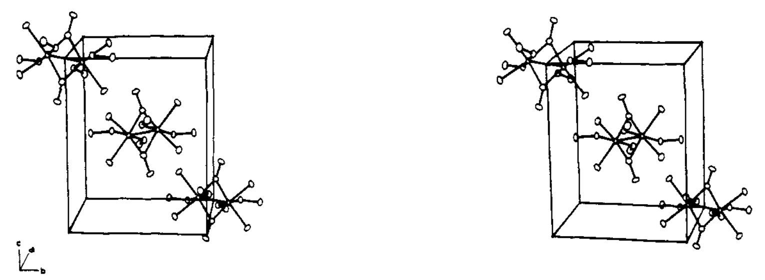

Figure 4. A stereoscopic view of the unit cell of $W_2Cl_4(OCH_3)_4(HOCH_3)_2$ (**1**).

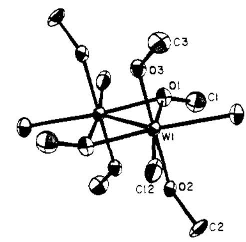

Figure 5. An ORTEP diagram of **1** with thermal ellipsoids at the 40% probability level.

ically irreversible follows from the observation that the $i_{p,a}:i_{p,c}$ ratio is <1 and that a product wave appears at $E_{p,a} = -0.26$ V in the anionic sweep following the reduction. Electrolysis of a solution at −1.0 V leads to decomposition. On the other hand, upon electrolysis at +1.0 V (i.e., anionic relative to the irreversible oxidation) the solution color changes from green to orange-red and the resultant cyclic voltammogram corresponds to that of the singly bonded ditungsten complex $W_2Cl_4(OEt)_6$.[12] We have found that this latter complex can be prepared in good yield by the chemical oxidation of $W_2Cl_4(OEt)_4(EtOH)_2$ by using either silver nitrate or molecular oxygen, the full details of which are described elsewhere.[12] The cyclic voltammogram of a dichloromethane solution of $W_2Cl_4(OEt)_6$ is shown in Figure 3b, being characterized by reductions at $E_{1/2} = -0.76$ V ($i_{p,a}:i_{p,c} \approx 1$) and $E_{p,c} = -1.32$ V vs. SCE. The reduction at −0.76 V is a one-electron process as judged by a comparison of the peak currents with those for the ferrocene–ferrocinium couple in a solution containing equimolar quantities of $(C_5H_5)_2Fe$ and $W_2Cl_4(OEt)_6$.

The facile oxidation of $W_2Cl_4(OEt)_4(EtOH)_2$ to $W_2Cl_4(OEt)_6$ provides an explanation for the results we obtained upon measuring the mass spectrum (at 150 °C) of the tungsten(IV) complex. The only species detected were those which characterize the mass spectrum of $W_2Cl_4(OEt)_6$,[12] the parent ion peaks being clustered around *m/e* 780. This tungsten(V) complex is apparently formed in very small amounts from the thermal decomposition of $W_2Cl_4(OEt)_4(EtOH)_2$.[13]

Structures. The crystal structure of $W_2Cl_4(OCH_3)_4(HOCH_3)_2$ (**1**) consists of a well-separated arrangement of molecules situated on crystallographic inversion centers in the unit cell (Figure 4). The individual molecules consist of two edge-sharing distorted octahedra. The molecular structure and atomic numbering scheme are presented in Figure 5, illustrated in a view looking obliquely to the metal–metal bond.

The octahedral coordination sphere of each tungsten atom consists of two cis-chlorine ligands and two cis-bridging methoxide ligands forming the equatorial plane while one methoxide group and one methanol molecule fill the axial positions. The metal–metal vector bisects the edge formed by the bridging oxygen atoms and the complete $Cl_2W(\mu\text{-}O)_2WCl_2$ unit is planar. As expected, the plane defined by the two metal atoms and the oxygen atoms of the axial ligands makes a dihedral angle of 90.0° with the $W_2Cl_4(\mu\text{-}O)_2$ unit. However, because of the inequality of the independent W–O(terminal) bond distances, the central $W_2(\mu\text{-}O)_2O_4Cl_4$ unit has only the imposed crystallographic symmetry.

Table VII. Bond Distances (Å) and Bond Angles (Deg) for $W_2Cl_4(OCH_3)_4(HOCH_3)_2$ (1)

A. Distances

W(1)–W(1)	2.481 (1)	W(1)–O(3)	1.950 (5)
W(1)–Cl(1)	2.382 (2)	O(1)–C(1)	1.453 (11)
W(1)–Cl(2)	2.389 (2)	O(2)–O(3)′	2.483 (7)
W(1)–O(1)	2.032 (6)	O(2)–C(2)	1.474 (10)
W(1)–O(1)′	2.036 (6)	O(3)–C(3)	1.482 (10)
W(1)–O(2)	2.036 (6)		

B. Angles

W(1)′–W(1)–Cl(1)	135.01 (7)	Cl(2)–W(1)–O(2)	89.2 (2)
W(1)′–W(1)–Cl(2)	135.21 (7)	Cl(2)–W(1)–O(3)	90.3 (2)
W(1)′–W(1)–O(1)	52.5 (2)	O(1)–W(1)–O(1)′	104.8 (2)
W(1)–W(1)′–O(1)′	52.3 (2)	O(1)–W(1)–O(2)	89.8 (2)
W(1)′–W(1)–O(2)	88.9 (2)	O(1)–W(1)–O(3)	90.7 (2)
W(1)′–W(1)–O(3)	91.1 (2)	O(1)′–W(1)–O(3)	88.9 (2)
Cl(1)–W(1)–Cl(2)	89.71 (9)	O(1)′–W(1)–O(3)	90.7 (2)
Cl(1)–W(1)–O(1)	82.6 (2)	O(2)–W(1)–O(3)	179.4 (2)
Cl(1)–W(1)–O(1)′	172.4 (2)	W(1)–O(1)–W(1)′	75.2 (2)
Cl(1)–W(1)–O(2)	89.5 (2)	W(1)–O(1)–C(1)	132.5 (6)
Cl(1)–W(1)–O(3)	90.9 (2)	W(1)′–O(1)–C(1)	130.1 (6)
Cl(2)–W(1)–O(1)	172.2 (2)	W(1)–O(2)–C(2)	130.1 (5)
Cl(2)–W(1)–O(1)′	82.9 (2)	W(1)–O(3)–C(3)	131.3 (5)

Many of the observed distances and angles (Table VII) are similar to those found in $W_2Cl_4(OCH_2CH_3)_6$. The average W–Cl bond length of 2.386 (4) Å in **1** is comparable to that of 2.403 (7) Å in the W(V) compound. The W–O(bridging) distances average 2.034 (6) Å while the W–O(terminal) bond lengths are 1.950 (5) and 2.036 (6) Å. The O–C distances average 1.47 (2) Å. The W–W bond distance is 2.481 (1) Å which is 0.234 Å shorter than the analogous distance in the hexaalkoxide W(V) species.

The molecular structure of the ethyl derivative $W_2Cl_4(OCH_2CH_3)_4(HOCH_2CH_3)_2$ (**2**) is very similar to that of **1**. Although it resides on a general position in the unit cell (shown in Figure 6), the geometry of the internal $W_2Cl_4(\mu\text{-}O)_2O_4$ unit has near inversion symmetry. A representation of the molecule depicting the atomic numbering scheme is given in Figure 7.

The four independent W–Cl bond lengths (Table VIII) are statistically equivalent and average 2.390 (3) Å, a distance which is equivalent to that found in **1**. Th W–O(bridging) distances average 2.022 (8) Å and are not significantly different from these in the methoxide compound. The two different W–O(terminal) distances average 1.962 (7) and 2.020 (4) Å. The average distances for the O–C and C–C bonds are 1.46 (2) and 1.48 (1) Å, respectively. The W–W bond length in this complex, 2.483 (2) Å, is statistically identical with the corresponding distance observed for **1**.

The structures of **1** and **2** are as similar as they could be, neglecting the presence of the β-carbon atoms in **2**. The bond lengths and angles common to both structures are listed side by side and the averages given in Table IX. A careful examination and interpretation of the characteristic features leads to important conclusions concerning the composition and bonding in molecules of this class.

The ambiguity that has previously prevailed concerning composition has already been summarized and the nonstructural evidence in favor of the $W_2Cl_4(OR)_4(ROH)_2$ formula marshalled.

---

[13] We carried out the thermal decomposition $W_2Cl_4(OEt)_4(EtOH)_2$ in vacuo at temperatures up to 200 °C. This green complex turned black but did not under any conditions form significant amounts of $W_2Cl_4(OEt)_6$. Only a trace of sublimable material was formed during the decomposition.

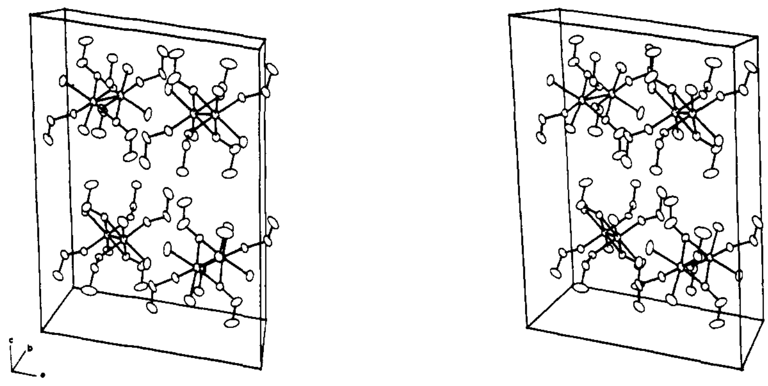

Figure 6. A stereoscopic view of the unit cell of $W_2Cl_4(OCH_2CH_3)_4(HOCH_2CH_3)_2$ (**2**).

Table VIII. Bond Distances (Å) and Bond Angles (Deg) for $W_2Cl_4(OCH_2CH_3)_4(HOCH_2CH_3)_2$ (2)

	A. Distances		
W(1)-W(2)	2.483 (1)	O(1)-C(1)	1.44 (1)
-Cl(3)	2.389 (3)	O(2)-C(3)	1.44 (1)
-Cl(4)	2.391 (2)	O(3)-C(5)	1.49 (1)
-O(1)	2.021 (5)	O(4)-C(7)	1.46 (1)
-O(2)	2.023 (6)	O(5)-C(9)	1.46 (1)
-O(5)	2.016 (6)	O(6)-C(11)	1.48 (1)
-O(6)	1.968 (6)	C(1)-C(2)	1.44 (2)
W(2)-Cl(1)	2.387 (3)	C(3)-C(4)	1.49 (2)
-Cl(2)	2.391 (3)	C(5)-C(6)	1.50 (2)
-O(1)	2.030 (6)	C(7)-C(8)	1.49 (2)
-O(2)	2.015 (6)	C(9)-C(10)	1.50 (2)
-O(3)	1.955 (6)	C(11)-C(12)	1.47 (2)
-O(4)	2.023 (5)	O(3)-O(5)	2.488 (8)
		O(4)-O(6)	2.489 (7)
	B. Angles		
W(2)-W(1)-Cl(3)	136.55 (8)	W(1)-W(2)-O(2)	52.2 (2)
-Cl(4)	135.79 (8)	-O(3)	90.8 (2)
-O(1)	52.4 (2)	-O(4)	89.7 (2)
-O(2)	51.9 (2)	Cl(1)-W(2)-Cl(2)	88.2 (1)
-O(5)	89.3 (2)	-O(1)	83.6 (2)
-O(6)	90.5 (2)	-O(2)	172.2 (2)
Cl(3)-W(1)-Cl(4)	87.6 (1)	-O(3)	90.4 (2)
-O(1)	84.2 (2)	-O(4)	89.3 (2)
-O(2)	171.4 (2)	Cl(2)-W(2)-O(1)	171.3 (2)
-O(5)	89.4 (2)	-O(2)	84.0 (2)
-O(6)	91.1 (2)	-O(3)	91.1 (2)
Cl(4)-W(1)-O(1)	171.8 (2)	-O(4)	88.5 (2)
-O(2)	83.9 (2)	O(1)-W(2)-O(2)	104.2 (2)
-O(5)	89.4 (2)	-O(3)	91.5 (2)
-O(6)	90.4 (2)	-O(4)	88.9 (2)
O(1)-W(1)-O(2)	104.3 (2)	O(2)-W(2)-O(3)	90.1 (2)
-O(5)	90.8 (2)	-O(4)	90.1 (2)
-O(6)	89.6 (2)	O(3)-W(2)-O(4)	179.5 (2)
O(2)-W(1)-O(5)	89.0 (2)	W(1)-O(1)-W(2)	75.6 (2)
-O(6)	90.4 (2)	-C(1)	133.0 (7)
O(5)-W(1)-O(6)	179.4 (2)	W(2)-O(1)-C(1)	131.6 (8)
W(1)-W(2)-Cl(1)	135.60 (9)	W(1)-O(2)-W(2)	75.9 (2)
-Cl(2)	136.19 (9)	-C(3)	131.8 (7)
-O(1)	52.0 (2)	W(2)-O(2)-C(3)	135.0 (6)
W(2)-O(3)-C(5)	130.3 (6)	O(2)-C(3)-C(4)	117 (1)
W(2)-O(4)-C(7)	130.9 (5)	O(3)-C(5)-C(6)	108 (1)
W(1)-O(5)-C(9)	130.1 (5)	O(4)-C(7)-C(8)	108.2 (9)
W(1)-O(6)-C(11)	130.2 (6)	O(5)-C(9)-C(10)	109.6 (8)
O(1)-C(1)-C(2)	113 (1)	O(6)-C(11)-C(12)	108.8 (9)

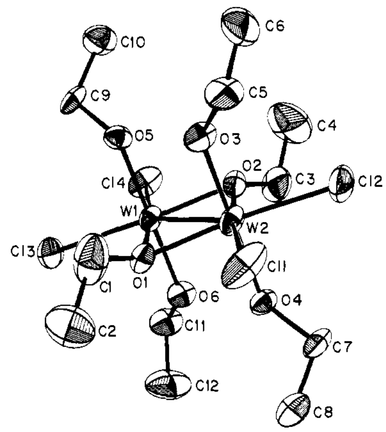

Figure 7. An ORTEP diagram of **2** with thermal ellipsoids at the 40% probability level.

Table IX. Comparison of Bond Lengths (Å) and Angles (Deg) in the Two Structures

	average values		
	$W_2Cl_4(OMe)_4$-$(MeOH)_2$	$W_2Cl_4(OEt)_4$-$(EtOH)_2$	grand av
W-W	2.481 (1)	2.483 (1)	2.482 (1)
W-Cl	2.386 (2)	2.390 (3)	2.388 (2)
W-OR(bridged)	2.034 (6)	2.022 (8)	2.028 (6)
W-OR(terminal)	1.950 (5)	1.962 (6)	1.956 (5)
W-O(H)R	2.036 (6)	2.020 (5)	2.028 (8)
C-O	1.47 (2)	1.46 (2)	1.46 (1)
C-C		1.48 (1)	1.48 (1)
O···O	2.483 (7)	2.488 (6)	2.485 (7)
W-O-C	131.1 (5)	130.3 (5)	130.7 (5)
W-O(H)-C	130.1 (5)	130.5 (5)	130.3 (5)
Cl-W-Cl	89.7 (1)	87.9 (3)	88.8 (9)
W-W-O(terminal)	91.1 (2)	90.0 (6)	90.6 (6)

We turn now to the structural evidence concerning composition. The several different W–O bond lengths form a pattern consistent with only one arrangement of RO and ROH terminal ligands, as the following arguments will show.

The W–O(br) distances, which average 2.03 (1) Å, are in the range observed for $W_2Cl_4(OEt)_6$[12] and $Nb_2(OMe)_{10}$.[14] In these two cases there is no uncertainty about the fact that we have bridging RO and not ROH groups. It is interesting that M–O(br) distances remain relatively constant even though the M–M bond orders that are bridged vary over the range 0–2.

As expected from the results for $W_2Cl_4(OEt)_6$ and $Nb_2(OMe)_{10}$ and other compounds, terminal W–OR bonds should be much shorter than the W–O(br) bonds. On the other hand terminal W–O(H)R bonds should be appreciably longer than terminal W–OR bonds. We see from Table IX that on each tungsten atom we have one terminal W–O bond appreciably shorter than the W–O(br) bonds, 1.96 vs. 2.03 Å, and one longer terminal W–O bond, which, by coincidence is about the same length as the W–O(br) bonds. These should correspond to the terminal W–OR and W–O(H)R bonds, respectively.

It will be noticed, however, that the terminal W–OR bonds are not as short as might have been expected from $W_2Cl_4(OEt)_6$, where they are 1.82 Å. This has a very natural explanation, as indicated in Figure 8. In the $W_2Cl_4(OR)_4(ROH)_2$ compounds

---

(14) Pinkerton, A. A.; Schwarzenbach, D.; Hubert-Pfalzgraf, L. G.; Riess, J. G. *Inorg. Chem.* **1976**, *15*, 1196.

(15) Shaik, S.; Hoffmann, R.; Fisel, C. R.; Summerville, R. H. *J. Am. Chem. Soc.* **1980**, *102*, 4555.

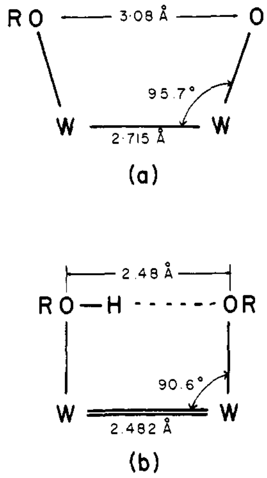

Figure 8. Schematic comparison of the arrangements of the syn axial ligands in $W_2Cl_4(OR)_6$ and $W_2Cl_4(OR)_4(ROH)_2$ compounds.

we have, at syn axial positions, OR on one W atom and HOR on the other. The W–O bonds stand essentially perpendicular to the equatorial plane instead of bending away from each other as a result of O···O repulsion. The reason for this must be that there is a hydrogen bond between them and, at an O···O distance of only 2.48 Å, this is quite a strong hydrogen bond and it may well tend toward being symmetric. As a result the limiting OR and HOR characters of the two syn ligands are compromised toward some intermediate character, and this causes the "W–OR" bond to be longer and the "W–O(H)R" bond to be shorter than would be expected for the pure limiting cases.

The hydrogen atoms in the hydrogen bonds were not detected in any of the electron density maps. This is not at all unusual and, in our experience, has always been the case. Residual electron density well localized around the proton is evidently (and not unexpectedly) very small in such a hydrogen-bonded situation and is insufficient to be detected. That there are hydrogen bonds between the syn oxygen atoms is an inescapable conclusion since the O···O distances of only 2.48 Å would be inexplicable in any other way.

The equations of a number of molecular planes, the dihedral angles between them, and the deviations of certain atoms from then have been calculated. The results are presented in Tables X and XI, which are available as supplementary material. The most important results of these calculations are the following. First, for the syn sets of $C_\alpha OWWOC_\alpha$ atoms shown in Figure 8b there is a close approach to coplanarity, as would be necessary if hydrogen bonds are to exist between the oxygen atoms. This can be expressed in terms of the dihedral angles between W–O–C_α planes and the O–W–W–O planes to which they are adjoined. For all such dihedral angles, of which there are six crystallographically independent ones in the two compounds, the average value is 5°, with the range being from 11.8° to 0.6°.

Second, the bridging oxygen atoms form pyramidal sets of bonds. This can be seen from the fact that the sum of the angles about each one is considerably less than 360°, namely, 338 (1)°, 340 (2)°, and 343 (2°) about O(1) of **1**, O(1) of **2**, and O(2) of **2**, respectively. Direct calculations of the deviations of the α-carbon atoms from the W–O–W planes give values of 0.75–0.78 Å.

Discussion

While the compounds described here are interesting from several points of view, we have found them especially interesting because of the metal–metal bonding. Taken together with the previously reported[12] $W_2Cl_4(OR)_6$ they provide an unusually good opportunity to make a detailed study of M–M single and double bonding in the structural context of a doubly bridged system. The number of extraneous compositional and structural changes on going from the singly to the doubly bonded systems, $W_2Cl_4(OR)_6$ to $W_2Cl_4(OR)_4(ROH)_2$, are as minimal as one could imagine: compositionally, only two hydrogen atoms are added, and structurally, aside from the buttressing effect of the two hydrogen bonds, all changes are those caused by the increase in M–M bond order from 1 to 2.

The fact that the W–W distance changes from 2.715 to 2.482 Å in an essentially identical structural context as we go from $W_2Cl_4(OR)_6$ to $W_2Cl_4(OR)_4(ROH)_2$ may reasonably be called prima facie evidence that the W–W bond order has increased. When the metal atom electronic configurations, d^1–d^1 and d^2–d^2, respectively are noted, and it is also recognized that in $W_2Cl_4(OR)_6$ the structural and magnetic evidence imply the presence of a W–W single bond, the bond order increase must surely be from 1 to 2. Moreover, qualitative considerations would suggest that the double bond would consist of the σ component responsible for the d^1–d^1 single bond plus a π bond. The Fenske–Hall calculations were carried out to provide a more quantitative and more detailed picture of this bonding.

Molecular Orbitals. No previous computations have been reported on such a system and even qualitative discussions are rare. The comprehensive paper by Shaik, Hoffmann, Fisel, and Summerville[15] deals with only one d^2–d^2 system, Re_2Cl_{10}, and this is a nonbonded one. In general, the interest of Hoffmann et al. was focused on larger bridging groups, Cl^-, PR_2^-, or SR^-, although CO and CH_2 were given some attention. Needless to say, of course, the nature of the OR-bridged species and the results of our calculations merge without discontinuity into the content of the Hoffmann paper, and the two studies complement each other. For example, in the part of their Figure 2 dealing with the Re_2Cl_{10} case, they foresaw that at Re–Cl–Re angles below about 75°, Re=Re double bonding might be expected, with a $b_{1u}(\pi)$ orbital as the HOMO and an $a_g(\sigma)$ orbital next below it. In reality, of course, Re_2Cl_{10} has a 98.1° angle, the Re–Re distance is 3.74 Å and there is no indication of direct bonding between the metal atoms. The advantage enjoyed by the $W^{IV}(\mu\text{-}OR)_2W^{IV}$ systems is twofold: (1) the bridging oxygen atom is so much smaller than Cl that the tungsten atoms can approach each other closely without excessively reducing the angle at the bridging group; (2) the potential repulsions between adjacent axial ligands are eliminated by the formation of hydrogen bonds between syn RO and ROH groups as discussed above.

We may begin our discussion of the complete computational results by examining Table V in which the MO's are listed in order of energy, and each one is identified by its serially numbered symmetry type, according to the C_{2h} symmetry used. In addition, the provenance of these MO's is shown. For the contributions made by ligand atoms, only a total percentage for all ligand AO's is given. For the metal atoms the contributions from the members of the subset of Mo_2^{8+} MO's, the M_i, are stated, with a further designation of which atomic d orbitals of the metal atoms are mainly involved.

The results of the calculation on the entire $Mo_2Cl_4(OH)_4(H_2O)_2$ molecule and the relationship of these results to the Mo_2^{8+} orbitals and the ligand orbitals are shown in Figure 2. Two columns are used for the MO's of the complex: shown on the right are all MO's listed in Table V and, on the left, only those MO's with >10% metal character.

The HOMO, $11b_u$, has the principal function of providing a π bond between the metal atoms. It receives its major contribution from the M_2 orbital which is itself made up 99% from molybdenum d_{xz} atomic orbitals. There are minor contributions from chlorine and $O_b(p\pi)$ orbitals. A schematic picture of the $11b_u$ orbital is given in Figure 9. Besides the 77% contribution that M_2 makes to the $11b_u$ MO, it makes small contributions to two of the lower b_u MO's, viz., $9b_u$ (12%) and $6b_u$ (8%). The $9b_u$ orbital is essentially (82%) a chlorine lone-pair orbital while the $6b_u$ is mainly (80%) a lone-pair orbital on the bridging oxygen atoms. The Mulliken population of the M_2 orbital (1.98) multiplied by 0.77 and divided by 2 gives us an Mo–Mo π-bond order from the $11b_u$ orbital alone, of 0.762.

The Mo–Mo σ bonding is more widely dispersed. We find M_1 turning up mainly in $10a_g$ (48%) and $7a_g$ (30%). The first of these also has a major contribution from the chlorine atoms but in an antibonding sense, as shown schematically in Figure 9. The $7a_g$

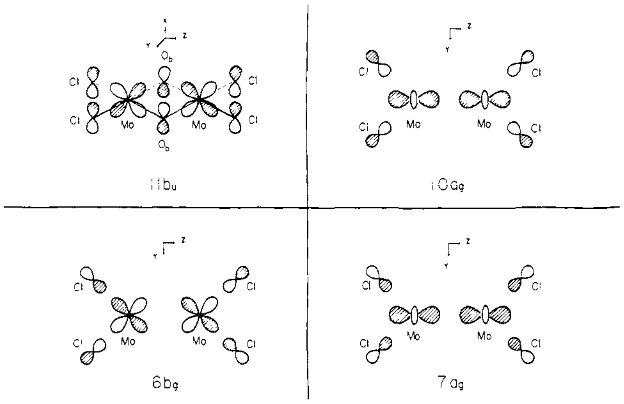

Figure 9. Schematic sketches of several molecular orbitals that are of major interest in the M-M bonding.

MO has its main contribution from chlorine σ orbitals and is more an Mo–Cl σ-bonding orbital than an Mo–Mo σ-bonding orbital, as also shown in Figure 9. The combined Mo–Mo σ-bond order obtained from the $10a_g$ and $7a_g$ MO's is 0.707. The sum of the contributions from M_1 and M_2 to Mo–Mo bonding in the entire $Mo_2Cl_4(OH)_4(H_2O)_2$ molecule is 1.47, whereas the total Mo–Mo bond order, obtained by summing all contributions is 1.65. It is, therefore, reasonable to say in a semiquantitative way that we have an Mo–Mo σ bond which receives contributions from the $7a_g$ and $10a_g$ MO's and an Mo–Mo π bond, in a plane perpendicular to the central $Cl_2Mo(\mu\text{-}O)_2MoCl_2$ plane, which is almost entirely attributable to the $11b_u$ MO.

Only one other MO has a contribution greater than 16% from any one M_i and that is the $6b_g$ orbital, which has a 26% contribution from M_9. It also has 65% contribution from chlorine AO's, and, as shown schematically in Figure 9, it is principally an Mo–Cl σ-bonding orbital, with slightly antibonding in-plane π character with respect to the Mo–Mo interaction.

Relationship of These Complexes to Other Multiply Bonded Dinuclear Complexes. The oxidation of derivatives of the W_2^{4+} core to $W_2Cl_4(OR)_4(ROH)_4$ corresponds to a decrease in the W–W bond order from 4 to 2. Since we have previously demonstrated[3] that the conversion of $W_2(mhp)_4$ to $W_2Cl_4(OR)_4(ROH)_2$ proceeds via the triply bonded $[W_2Cl_9]^{3-}$ anion, and with our discovery[12] that the tungsten(IV) species can be oxidized to $W_2Cl_4(OEt)_6$, we have a series of complexes $W_2(mhp)_4$ and $W_2(dmhp)_4$, $[W_2Cl_9]^{3-}$, $W_2Cl_4(OR)_4(ROH)_2$, and $W_2Cl_4(OR)_6$, in which the metal–metal order decreases from 4 to 3 to 2 to 1. Such an extensive sequence of bond order changes for a given pair of metal atoms is still very rare in the chemistry of multiply bonded dinuclear complexes.[7]

Interestingly, another class of tungsten(IV) alkoxides is known but these are structurally dissimilar from $W_2Cl_4(OR)_4(ROH)_2$. The triply bonded dinuclear complex $W_2(NMe_2)_6$ is oxidized by methanol and ethanol to the tetrameric $W_4(OR)_{16}$ compounds.[16] These molecules do not possess the localized W–W double bonding of $W_2Cl_4(OR)_4(ROH)_2$.

Our results also bear comparison with recent molybdenum alkoxide chemistry.[17] The triply bonded isopropoxide $Mo_2(O\text{-}i\text{-}Pr)_6$ can be oxidized to $Mo_2X_4(O\text{-}i\text{-}Pr)_6$ upon reaction with the halogens (Cl_2, Br_2, and I_2). The formation of these complexes, which are isostructural with $W_2Cl_4(OEt)_6$,[12] probably proceeds via the intermediate and very unstable molybdenum(IV) complexes $Mo_2X_2(O\text{-}i\text{-}Pr)_6$,[17] species which may contain a Mo=Mo bond. However, a much better characterized complex which exhibits double bonding is $Mo_2(O\text{-}i\text{-}Pr)_8$, which can be formed, amongst other ways, by the oxidative addition of i-PrOO-i-Pr to $Mo_2(O\text{-}i\text{-}Pr)_6$.[17] Since the tetraalkoxides of tungsten(IV) are tetramers[16] (vide supra), the dinuclear complexes $W_2Cl_4(OR)_4(ROH)_2$ are the closest structural analogues of the hypothetical $W_2(OR)_8$.

Relevance to Some Solid-State Structures. The experimental results and calculations for the $W_2Cl_4(OR)_4(ROH)_2$ molecules are relevant to several cases of metal-metal interaction found in metal oxides and mixed-metal oxides in the solid state, where instead of discrete dinuclear units there are infinitely extended arrays with recognizable dinuclear components. The most immediately obvious example in this context is WO_2, which has long been known[18] to have a modified rutile structure in which alternate W–W distances, across shared edges of WO_6 octahedra, are 2.475 (2) Å (while the others are 3.096 (2) Å). The postulate that W=W double bonds join the close pairs is strongly supported by the present results. The same would be true of the isostructural[19] MoO_2 where the short and long Mo–Mo distances are 2.5106 (5) and 3.118 (5) Å, respectively. Previous theoretical work on the electronic structure[20] of MoO_2 has dealt with its superconductivity, and the results are not inconsistent with the existence of a double bond. The weak paramagnetism of MoO_2 has been investigated by neutron diffraction and attributed to Pauli paramagnetism of the collective electrons.[21]

Several rhenium compounds bear comparison with the present results. In $Nd_4Re_2O_{11}$ there are isolated Re_2O_{10} units, with an Re–Re distance of 2.421 (1) Å.[22] Since Re^V is a d^2 system like W^{IV}, we have here another likely example of a double bond between d^2 metal ions. In $La_4Re_6O_{19}$ there are Re_2O_{10} units linked by corner sharing, with an Re–Re distance of 2.422 (7) Å.[23,24] Here the oxidation number of rhenium, assuming La^{3+} ions, is $4^1/_3$, meaning that there are $5^1/_2$ electrons per Re_2O_{10} unit available for potential Re–Re bonding. A bond order of at least 2 would seem reasonable. Finally, there is the fascinating compound[25] $La_6Re_4O_{18}$ which contains Re_2O_8 units with Re–Re triple bonds (2.235 (6) Å) and also edge-sharing bioctahedra, Re_2O_{10}, in which the metal atoms are presumably Re^V. The Re–Re distance 2.456 (5) Å can be readily reconciled with the existence of a double bond.

Acknowledgment. We are grateful to the National Science Foundation for support at both universities and to The Robert A. Welch Foundation for support under Grant No. A-494 at Texas A&M University.

Supplementary Material Available: Tables of observed and calculated structure factors and of least-squares planes and dihedral angles (20 pages). Ordering information is given on any current masthead page.

---

(16) Chisholm, M. H.; Huffman, J. C.; Leonelli, J., submitted for publication.

(17) Chisholm, M. H.; Kirkpatrick, C. C.; Huffman, J. C., submitted for publication.

(18) Palmer, D. J.; Dickens, P. G. *Acta Crystallogr., Sect. B* **1979**, *B35*, 2199.

(19) Brandt, B. G.; Skapski, A. C. *Acta Chem. Scand.* **1967**, *21*, 661.

(20) Goodenough, J. B. *Bull. Soc. Chim. Fr.* **1965**, *4*, 1200.

(21) Ghose, J.; Greenwood, N. N.; Hallam, G. C.; Read, D. A. *J. Solid State Chem.* **1976**, *19*, 365.

(22) Wilhelmi, K. A.; Lagervall, E.; Muller, O. *Acta Chem. Scand.* **1970**, *24*, 3406.

(23) Morrow, N. L.; Katz, L. *Acta Crystallogr., Sect. B* **1968**, *B24*, 1466.

(24) Longo, J. M.; Sleight, A. W. *Inorg. Chem.* **1968**, *7*, 108.

(25) Besse, J.-P.; Baud, G.; Chevalier, R. *Acta Crystallogr., Sect. B* **1978**, *B34*, 3532.